

## Numeric reconstruction of 2D cellular actomyosin network from substrate displacement

Wagner Shin Nishitani\*, Ronny Calixto Carbonari, Adriano Mesquita Alencar

**Abstract Introduction:** One of the fundamental structural elements of the cell is the cytoskeleton. Along with myosin, actin microfilaments are responsible for cellular contractions, and their organization may be related to pathological changes in myocardial tissue. Due to the complexity of factors involved, numerical modeling of the cytoskeleton has the potential to contribute to a better understanding of mechanical cues in cellular activities. In this work, a systematic method was developed for the reconstruction of an actomyosin topology based on the displacement exerted by the cell on a flexible substrate. It is an inverse problem which could be considered a phenomenological approach to traction force microscopy (TFM). **Methods:** An actomyosin distribution was found with a topology optimization method (TOM), varying the material density and angle of contraction of each element of the actomyosin domain. The routine was implemented with a linear material model for the bidimensional actomyosin elements and tridimensional substrate. The topology generated minimizes the nodal displacement squared differences between the generated topology and experimental displacement fields obtained by TFM. The structure resulting from TOM was compared to the actin structures observed experimentally with a GFP-attached actin marker. **Results:** The optimized topology reproduced the main features of the experimental actin and its squared displacement differences were  $11.24 \mu\text{m}^2$ , 27.5% of the sum of experimental squared nodal displacements ( $40.87 \mu\text{m}^2$ ). **Conclusion:** This approach extends the literature with a model for the actomyosin structure capable of distributing anisotropic material freely, allowing heterogeneous contraction over the cell extension.

**Keywords:** Traction force microscopy, Cell mechanics, Actin, Topology optimization method, Finite element method.

### Introduction

One of the fundamental structural elements of the cell is the cytoskeleton. It is composed of microtubules, intermediate filaments and microfilaments. Microfilaments are composed of F-actin, filaments produced by polymerization of G-actin. Along with myosin, microfilaments are responsible for cellular contraction. The study of these filaments could be important because their organization may be related to pathological changes in myocardial tissue (Hiremath et al., 2014), as extracellular matrix (ECM) microstructure is related to alignment of cells and cytoskeleton morphology (Fernandez and Bausch, 2009; Rhee and Grinnell, 2007; Tomasek et al., 2002). Cells adhere to their substrate through integrins, transmembrane proteins which form focal adhesions. Integrins are proteins responsible for anchoring cells to the ECM and consequently for the transmission of forces applied by the cells to their substrate (Ingber, 2006).

Due to the complexity of factors involved, numerical modeling of the cytoskeleton has the potential to contribute to a better understanding of

mechanical cues in cellular activities. The utilization of simplified models helps to clarify which factors are really essential and which ones have only a marginal influence. The establishment of a systematic method for cytoskeleton reconstruction of a cell under investigation may accelerate the development of mathematical models by allowing a faster comparison of experimental data with numerical results, needed for model validation (Ghosh et al., 2011).

In this work, a systematic method was developed for the reconstruction of actomyosin topology based on the displacement exerted by the cell on a flexible substrate. The actomyosin topology is defined by a density and an angle of contraction for each element of the reconstruction domain, representing stress fibers present in the cell. It is an inverse problem, analogous to reconstructing a traction field from its displacement.

A definition for the actomyosin material contraction was the first step in the routine development. The actomyosin contraction was modeled by Sen et al. (2009) as an isotropic initial stress of the elements,

\*e-mail: [wagner.nishitani@ufabc.edu.br](mailto:wagner.nishitani@ufabc.edu.br)

Received: 30 April 2015 / Accepted: 30 October 2015

resulting in a homogeneous contraction in all directions. Chandran et al. (2009) proposed a simple model for a homogeneous isotropic actomyosin material which captures band-like propagation of stress fibers and relates a perpendicular force along with the known contractile axial force. In the present work, the actomyosin material is considered anisotropic, with the contraction modeled as an initial stress, but defined by an initial strain composed of  $x$  and  $y$  components according to an angle of contraction  $\theta$  that varies over the actomyosin domain.

The inverse nature of the problem justifies the use of the topology optimization method (TOM), whose applications include electric impedance tomography (Mello et al., 2008), for example. TOM consists of an iterative application of an optimization method followed by an analysis method to obtain the optimal distribution of material in the fixed domain. Thus, this method was used to obtain a cytoskeletal actomyosin distribution from the cell-generated flexible substrate displacement, measured experimentally with traction force microscopy (TFM). The structure resulting from TOM was compared to the actin structures observed experimentally. This technique utilizes images of fluorescent microbeads embedded on the substrate surface, acquired before and after the cells were removed from the substrate. The postprocessing of these images yields a displacement field and the traction responsible for generating it (Dembo and Wang, 1999). The present work could be considered a phenomenological approach to TFM, as it distributes the actomyosin structure necessary for producing the traction and displacement field observed experimentally.

## Methods

### Cell culture

Rabbit aortic smooth muscle (RASM), kindly provided by Prof. José Eduardo Krieger (Instituto do Coração da Faculdade de Medicina da Universidade de São Paulo, InCor-HC-FMUSP), were cultured in T-25 flasks (Corning, 430639) at 37°C in 5% CO<sub>2</sub> (21% O<sub>2</sub>, 74% N<sub>2</sub>). The growth medium was composed of Dulbecco's modified Eagle medium (DMEM) supplemented with 10% fetal bovine serum (FBS) and 1% antibiotic-antimycotic (Gibco, 15240). To visualize actin fibers, the cells were transfected with pCMV LifeAct-TagGFP2 plasmid (ibidi, 60101), an actin marker fused to a green fluorescent protein (GFP) developed by Riedl et al. (2008, 2010), kindly provided by Prof. Marinilce Fagundes dos Santos (Instituto de Ciências Biomédicas da Universidade de São Paulo, ICB-USP).

### Flexible substrate

The flexible substrates were made of polyacrylamide gel, whose preparation was based on protocols already established (Lo et al., 2000). The substrates had a Young modulus of 4.8 kPa and were made of acrylamide at 7.5% and Bis at 0.054%. Their thickness was about 50  $\mu\text{m}$  with a very thin layer of polyacrylamide with 0.2  $\mu\text{m}$  fluorescent microbeads (Molecular Probes, F-8810) (Bridgman et al., 2001). The substrate surface was then activated with Sulfo-SANPAH (Thermo Scientific, 22589), according to the supplier protocol, and incubated overnight at 4°C with 200  $\mu\text{l}$  of collagen I (BD, rat-tail) at 0.2 mg/ml (0.035 mg/cm<sup>2</sup>).

### Traction force microscopy

The displacement field generated by the cell attached to a flexible substrate was obtained as part of a TFM experiment, already described in the literature (Dembo and Wang, 1999), which consisted of acquiring images of the substrate fluorescent microbeads before and after the cells were removed with trypsin-EDTA. The postprocessing of images to obtain the displacement and traction field was done with a plugin for ImageJ developed by Tseng et al. (2012), which is an approach similar to the one used by Butler et al. (2002) with additional regularization. Images from the marked actin were also acquired to verify the reconstruction results.

### Numerical reconstruction of actin-myosin

The algorithm was implemented with linear finite element method (FEM) for the displacement analysis. The substrate was modeled with a single layer of 8-node brick elements with the bottom surface constrained for no displacement. The actomyosin domain was modeled with 4-node bidimensional rectangular elements. Their nodal degrees of freedom were directly coupled to  $x$  and  $y$  degrees of freedom from the substrate top surface nodes. The present TOM implementation optimizes the material density  $\rho$  and angle of contraction  $\theta$  of the actomyosin structure over a bidimensional domain of rectangular elements, as shown in Figure 1.

The topology generated by TOM minimizes  $\Delta D$ , the sum of nodal displacement squared differences between the generated topology and experimental displacement fields, which is the objective function for this optimization problem:

$$\min_{\rho, \theta} \Delta D = \sum_{n=0}^{N_{\text{nodes}}} (u_n - \tilde{u}_n)^2 \quad (1)$$

where  $N_{\text{nodes}}$  is the number of nodes in the actomyosin domain, and  $u_n$  and  $\tilde{u}_n$  are the topology and experimental displacement of the node  $n$ .

The actomyosin density is represented by the material interpolation model “Simple Isotropic Material with Penalization” (SIMP) (Bendsøe and Sigmund, 1999), varying continuously between zero and one.

The formulation used in linear elastic bidimensional elements under plane stress or tridimensional elements was described by Zienkiewicz and Taylor (2000). The actomyosin contraction was modeled as an initial stress determined by an initial strain composed of

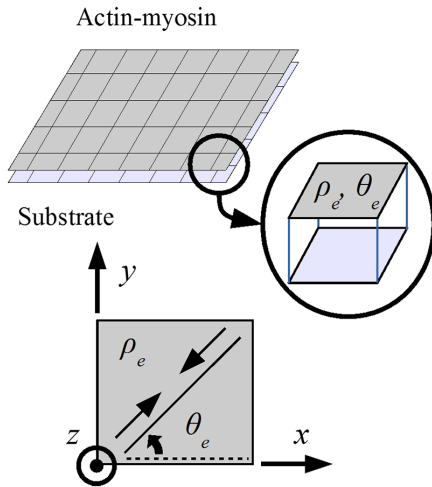


**Figure 1.** Domains of actin-myosin and substrate. Actomyosin element, rigidly linked to the substrate, and its variables (density  $\rho_e$  and angle of contraction  $\theta_e$ ).

$x$  and  $y$  components according to the angle  $\theta$  of each element. Contraction of the actomyosin structure was modulated by: 1) changing the material stiffness by varying its Young modulus and thickness of the bidimensional elements; 2) changing the initial strain. Actomyosin contraction is the result of the equilibrium between the initially stressed actomyosin and the substrate elements. An infinitely high stiffness of the actomyosin elements would cause a significant displacement even for densities  $\rho$  near zero, making it more difficult to visualize intermediate densities. Thus, it is important to test actomyosin parameters with material properties initially closer to those of the substrate.

The routine was implemented in Matlab R2009 (Mathworks), with the optimizer Globally Convergent Method of Moving Asymptotes (GCMMA) (Svanberg, 2002).

## Results

The TFM experiment yielded a brightfield and three fluorescent images: one of the marked actin and two of the substrate markers (microbeads). The postprocessing resulted in the displacement and traction fields. The brightfield, marked actin and postprocessing results are shown in Figure 2.

For the numerical reconstruction of the actomyosin topology, the Poisson’s ratio for the actomyosin

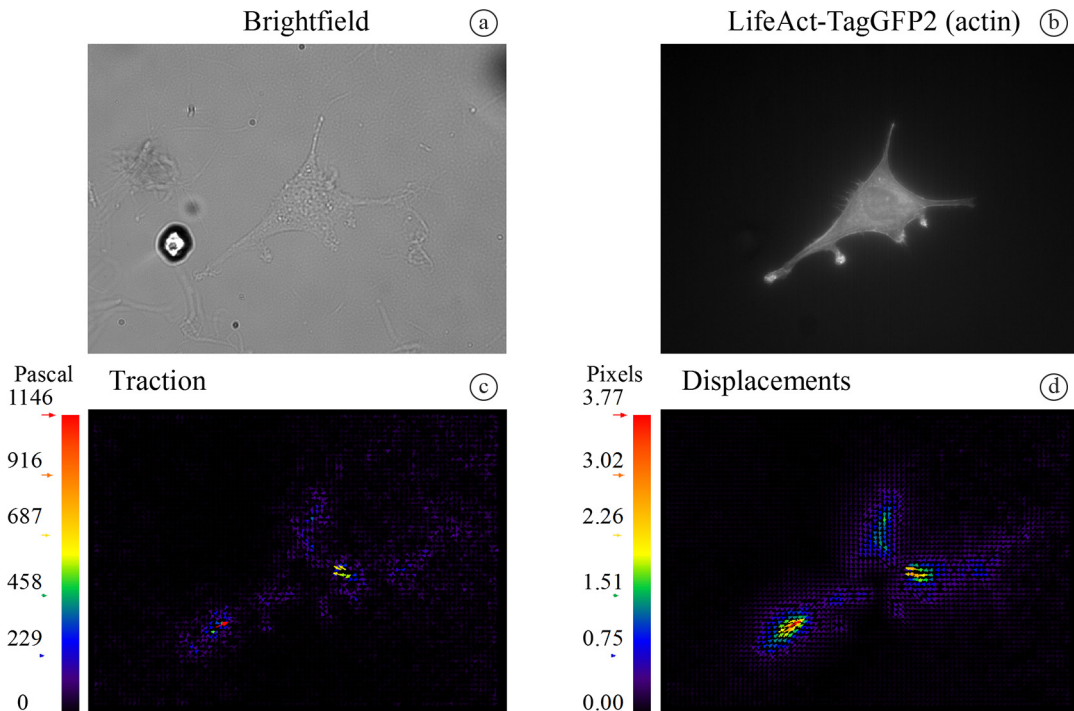


**Figure 2.** Traction force microscopy experimental results. (a) brightfield microscopy; (b) actin marked with LifeAct-TagGFP2; (c) displacement field; (d) traction field.

material was 0.3 (compressible) (Das and MacKintosh, 2010; Pelletier et al., 2009) and, for the substrate, 0.48 (almost incompressible) (Boudou et al., 2006). After some tests, the optimal Young modulus for the actomyosin material was 76.8 kPa, sixteen times the substrate Young modulus, and its optimal initial strain was 80%. The thickness of the actomyosin elements and of the substrate was 1 and 0.5  $\mu\text{m}$ , respectively. The optimized topology, along with its displacement field compared to the experimental data, are shown in Figure 3. As a quantification of the quality of the reconstruction, the sum of squared nodal displacement differences  $\Delta D$  was compared to the sum of experimental

squared nodal displacements. In this case,  $\Delta D$  was 11.24  $\mu\text{m}^2$ , 27.5% of the sum of experimental squared nodal displacements (40.87  $\mu\text{m}^2$ ).

## Discussion

The choice of element geometry and model of contraction had a significant impact in the routine capability to minimize the displacement differences. The use of rectangular elements for the actomyosin domain allowed a better representation of contractions in  $x$  and  $y$  directions relative to intermediate angles. The composition of an intermediate angle in terms

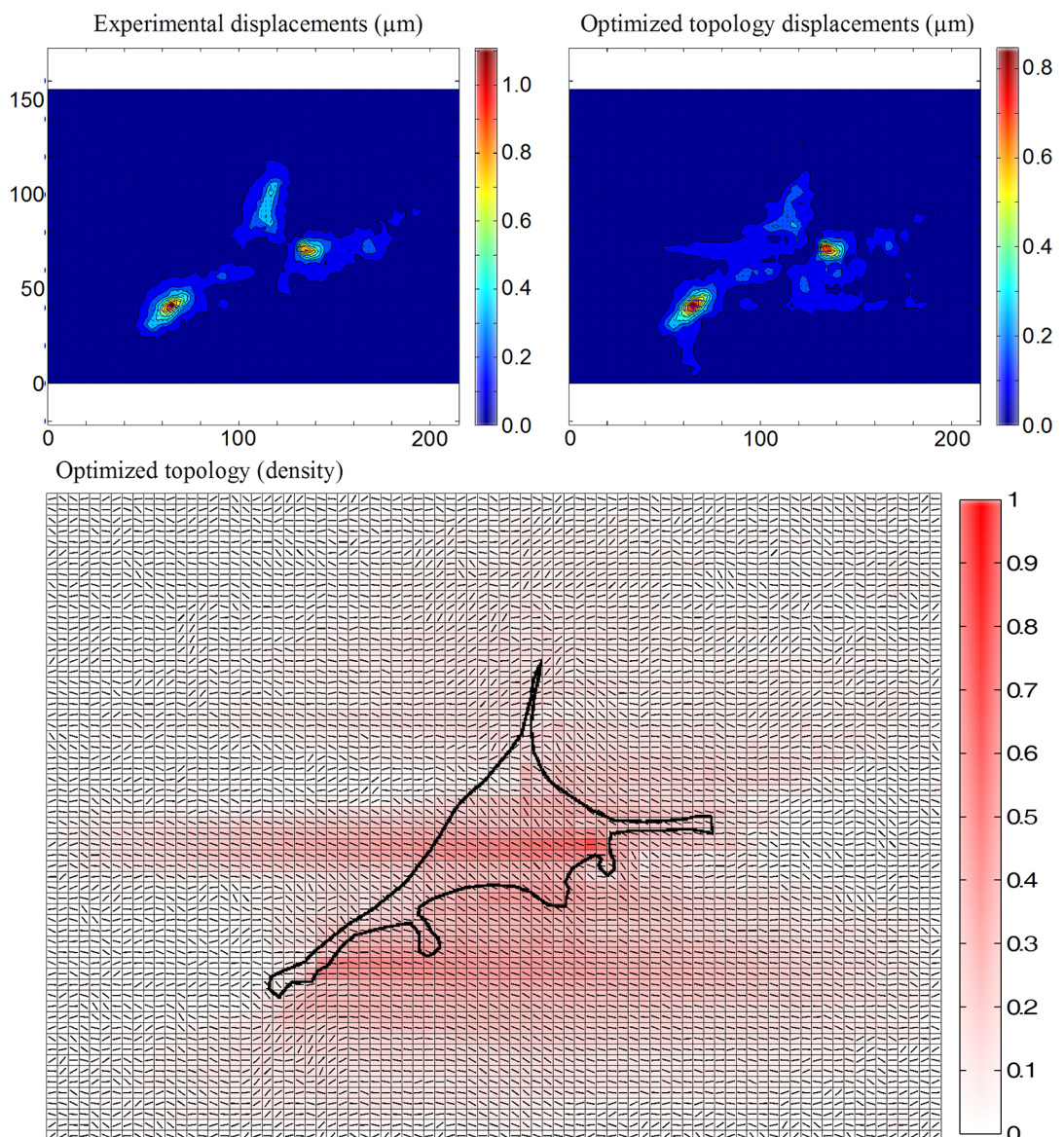


**Figure 3.** Numerical reconstruction of actomyosin structure with the boundaries of the cell, and comparison between experimental and reconstructed displacement fields.

of these orthogonal directions led to an identical contraction for the negative of that angle, which is something to be aware of when interpreting the results. Also, the contraction becomes isotropic for angles of  $45^\circ$  and  $-45^\circ$ .

Overall, the routine was capable of reproducing the main features of the experimental displacements. The denser actomyosin regions in the optimized topology correlated to regions covered by the cell. Regarding the actomyosin fiber orientation, the algorithm tends to orient them in the protrusion direction next to the cell boundary. In the inner regions, the optimized topology tends to contract more isotropically (angles closer to  $45^\circ$  or  $-45^\circ$ ). There are lower density regions in the topology outside the area covered by the cell, which can be explained by one of the assumptions of the model. It was assumed that the cells were adhered to the substrate all over their extension because the actomyosin domain nodes are directly coupled to the substrate top surface nodes. Thus, non-adhering actomyosin regions bridging adhered actomyosin portions of the cytoskeleton were replaced by lower density actomyosin distributed over a larger area, minimizing the sum of squared displacement differences ( $\Delta D$ ).

Some regions of the experimental cell were not represented in the optimized topology, which indicates that the cell is not using them actively to generate substrate displacement. This feature could be useful in studies in which the goal is to assess functionality among the actomyosin fibers.

The present work, despite considering an uniform initial strain for the actomyosin material model, allows local variations of fiber contractility due to differences in the material density distribution in the optimized topology. Also, the anisotropic nature of the actomyosin initial strain allows preferential contraction directions. Both aspects can contribute to existing models, which considered isotropic contractions over the cytoplasm (Sen et al., 2009), for example. The contraction model implemented does not incorporate the force perpendicular to the stress fibers proposed by Chandran et al. (2009), but it was still able to approximately reproduce experimental results. A refined actomyosin material model could improve this approximation.

As the algorithm targets the network of one particular cell, it utilizes more efficiently the experimental data available by not averaging the cell heterogeneity. In this work, the experimental data of one cell was analyzed to show the algorithm functionality.

In conclusion, an actomyosin numerical reconstruction routine was implemented with a linear material model for the bidimensional actomyosin elements

and tridimensional substrate. The optimized topology reproduced the main features of the experimental data. The present approach extends the literature with a model of the actomyosin structure capable of distributing anisotropic material freely, allowing heterogeneous contraction over the cell extension.

## Acknowledgements

We want to thank Prof. José Eduardo Krieger (Instituto do Coração da Faculdade de Medicina da Universidade de São Paulo, InCor-HC-FMUSP) for providing the RASM cells; Prof. Marinilce Fagundes dos Santos (Instituto de Ciências Biomédicas da Universidade de São Paulo, ICB-USP) for providing the pCMV LifeAct-TagGFP2 plasmid; São Paulo Research Foundation (FAPESP – grant #2012/07907-9); CAPES and CNPq.

## References

- Bendsøe MP, Sigmund O. Material interpolation schemes in topology optimization. *Archive of Applied Mechanics*. 1999; 69(9-10):635-54. <http://dx.doi.org/10.1007/s004190050248>.
- Boudou T, Ohayon J, Picart C, Tracqui P. An extended relationship for the characterization of Young's modulus and Poisson's ratio of tunable polyacrylamide gels. *Biorheology*. 2006; 43(6):721-8. PMID:17148855.
- Bridgman PC, Dave S, Asnes CF, Tullio AN, Adelstein RS. Myosin IIB is required for growth cone motility. *The Journal of Neuroscience*. 2001; 21(16):6159-69. PMID:11487639.
- Butler JP, Tolić-Nørrelykke IM, Fabry B, Fredberg JJ. Traction fields, moments, and strain energy that cells exert on their surroundings. *American Journal of Physiology. Cell Physiology*. 2002; 282(3):C595-605. <http://dx.doi.org/10.1152/ajpcell.00270.2001>. PMID:11832345.
- Chandran PL, Wolf CB, Mofrad MR. Band-like stress fiber propagation in a continuum and implications for Myosin contractile stresses. *Cellular and Molecular Bioengineering*. 2009; 2(1):13-27. <http://dx.doi.org/10.1007/s12195-009-0044-z>.
- Das M, MacKintosh F. Poisson's ratio in composite elastic media with rigid rods. *Physical Review Letters*. 2010; 105:138102. <http://dx.doi.org/10.1103/PhysRevLett.105.138102>.
- Dembo M, Wang YL. Stresses at the cell-to-substrate interface during locomotion of fibroblasts. *Biophysical Journal*. 1999; 76(4):2307-16. [http://dx.doi.org/10.1016/S0006-3495\(99\)77386-8](http://dx.doi.org/10.1016/S0006-3495(99)77386-8). PMID:10096925.
- Fernandez P, Bausch AR. The compaction of gels by cells: a case of collective mechanical activity. *Integrative Biology*. 2009; 1(3):252-9. <http://dx.doi.org/10.1039/b822897c>. PMID:20023736.
- Ghosh S, Matsuoka Y, Asai Y, Hsin K-Y, Kitano H. Software for systems biology: from tools to integrated platforms. *Nature Reviews. Genetics*. 2011; 12(12):821-32. PMID:22048662.

- Hiremath P, Bauer M, Aguirre AD, Cheng H-W, Unno K, Patel RB, Harvey BW, Chang W-T, Groarke JD, Liao R, Cheng S. Identifying early changes in myocardial microstructure in hypertensive heart disease. *PLoS One*. 2014; 9(5):e97424. <http://dx.doi.org/10.1371/journal.pone.0097424>. PMID:24831515.
- Ingber DE. Cellular mechanotransduction: putting all the pieces together again. *FASEB Journal: Official Publication of the Federation of American Societies for Experimental Biology*. 2006; 20(7):811-27. <http://dx.doi.org/10.1096/fj.05-5424rev>. PMID:16675838.
- Lo C-M, Wang H-B, Dembo M, Wang YL. Cell movement is guided by the rigidity of the substrate. *Biophysical Journal*. 2000; 79(1):144-52. [http://dx.doi.org/10.1016/S0006-3495\(00\)76279-5](http://dx.doi.org/10.1016/S0006-3495(00)76279-5). PMID:10866943.
- Mello LAM, Lima CR, Amato MBP, Lima RG, Silva ECN. Three-dimensional electrical impedance tomography: a topology optimization approach. *IEEE Transactions on Biomedical Engineering*. 2008; 55(2 Pt 1):531-40. <http://dx.doi.org/10.1109/TBME.2007.912637>. PMID:18269988.
- Pelletier V, Gal N, Fournier P, Kilfoil ML. Microrheology of microtubule solutions and actin-microtubule composite networks. *Physical Review Letters*. 2009; 102(18):188303. <http://dx.doi.org/10.1103/PhysRevLett.102.188303>. PMID:19518917.
- Rhee S, Grinnell F. Fibroblast mechanics in 3D collagen matrices. *Advanced Drug Delivery Reviews*. 2007; 59(13):1299-305. <http://dx.doi.org/10.1016/j.addr.2007.08.006>. PMID:17825456.
- Riedl J, Crevenna AH, Kessenbrock K, Yu JH, Neukirchen D, Bista M, Bradke F, Jenne D, Holak TA, Werb Z, Sixt M, Wedlich-Söldner R. Lifeact: a versatile marker to visualize F-actin. *Nature Methods*. 2008; 5(7):605-7. <http://dx.doi.org/10.1038/nmeth.1220>. PMID:18536722.
- Riedl J, Flynn KC, Raducanu A, Gärtner F, Beck G, Bösl M, Bradke F, Massberg S, Aszodi A, Sixt M, Wedlich-Söldner R. Lifeact mice for studying F-actin dynamics. *Nature Methods*. 2010; 7(3):168-9. <http://dx.doi.org/10.1038/nmeth0310-168>. PMID:20195247.
- Sen S, Engler AJ, Discher DE. Matrix strains induced by cells: computing how far cells can feel. *Cellular and Molecular Bioengineering*. 2009; 2(1):39-48. <http://dx.doi.org/10.1007/s12195-009-0052-z>. PMID:20582230.
- Svanberg K. A class of globally convergent optimization methods based on conservative convex separable approximations. *SIAM Journal on Optimization*. 2002; 12(2):555-73. <http://dx.doi.org/10.1137/S1052623499362822>.
- Tomasek JJ, Gabbiani G, Hinz B, Chaponnier C, Brown RA. Myofibroblasts and mechano-regulation of connective tissue remodelling. *Nature Reviews. Molecular Cell Biology*. 2002; 3(5):349-63. <http://dx.doi.org/10.1038/nrm809>. PMID:11988769.
- Tseng Q, Duchemin-Pelletier E, Deshiere A, Balland M, Guillou H, Filhol O, Théry M. Spatial organization of the extracellular matrix regulates cell-cell junction positioning. *Proceedings of the National Academy of Sciences of the United States of America*. 2012; 109(5):1506-11. <http://dx.doi.org/10.1073/pnas.1106377109>. PMID:22307605.
- Zienkiewicz OC, Taylor RL. The basis. 5th ed. Oxford: Butterworth-Heinemann; 2000. (The Finite Element Method; 1).

---

## Authors

**Wagner Shin Nishitani<sup>1,2\*</sup>, Ronny Calixto Carbonari<sup>2</sup>, Adriano Mesquita Alencar<sup>1</sup>**

<sup>1</sup> Physics Institute, Universidade de São Paulo – USP, Rua do Matão, 1371, Cidade Universitária, CEP 05508-090, São Paulo, SP, Brazil.

<sup>2</sup> Universidade Federal do ABC – UFABC, Santo André, SP, Brazil.